NANO-MICRO LETTERS ARTICLE
www.nmletters.org

Singular Sheet Etching of Graphene with Oxygen Plasma

Haider Al-Mumen[1,2,†], Fubo Rao[1,†], Wen Li[1,*], Lixin Dong[1,*]

(Received 03 September 2013; accepted 03 March 2014; published online 20 March 2014)

Abstract: This paper reports a simple and controllable post-synthesis method for engineering the number of graphene layers based on oxygen plasma etching. Singular sheet etching (SSE) of graphene was achieved with the optimum process duration of 38 seconds. As a demonstration of this SSE process, monolayer graphene films were produced from bilayer graphenes. Experimental investigations verified that the oxygen plasma etching removes a single layer graphene sheet in an anisotropic fashion rather than anisotropic mode. In addition, etching via the oxygen plasma at the ground electrodes introduced fewer defects to the bottom graphene layer compared with the conventional oxygen reactive ion etching using the powered electrodes. Such defects can further be reduced with an effective annealing treatment in an argon environment at 900-1000°C. These results demonstrate that our developed SSE method has enabled a microelectronics manufacturing compatible way for single sheet precision subtraction of graphene layers and a potential technique for producing large size graphenes with high yield from multilayer graphite materials.
Keywords: Graphene; Plasma; Singular sheet etching

Citation: Haider Al-Mumen, Fubo Rao, Wen Li and Lixin Dong, "Singular Sheet Etching of Graphene with Oxygen Plasma", Nano-Micro Lett. 6(2), 116-124 (2014). http://dx.doi.org/10.5101/nml.v6i2.p116-124

Introduction

The outstanding electronic, optical and physical properties [1-5] of graphene, atypical two-dimensional nano material have drawn tremendous attention from the scientific community for structuring electronic and photonic devices with higher performance in such applications as high-speed transistors, DNA sequencing, and biochemical sensors [6-10]. To date, significant progress has been made in producing graphene with both high yield and large size. Methods such as epitaxial synthesis [11], chemical vapor deposition [12,13], and chemical deoxidization [14] have been demonstrated for producing graphene of high quality. However, it is still a challenge for researchers to generate graphene with the desired number of graphene layers using the existing methods. Reproducible control of the number of graphene layers is highly desiredfor the reproducibility of graphene-based devices in practical applications as well as for the fundamental study of graphene characteristics. In particular, layer engineering of graphene will contribute greatly to the in-depth understanding of inter-layer transport properties in a multilayer structured graphene sensor previously developed in our group [15]. The influence of the number of graphene layers on graphene's electronic and optical properties has also been reported by other researchers [16]. To address this challenge, several efforts have been made towards realizing the layer engineering of graphene [17-20]. For example, Tour *et al.* [21] reported the layer-by-layer removal of graphene sheets using a wet etching method by coating graphene surfaces with zinc and dissolving the zinc with dilute acid, providing a promising method for engineering the number of graphene lay-

[1]Electrical & Computer Engineering, Michigan State University, Room 2120 Engineering Building, 428 S. Shaw Lane, East Lansing, MI 48824, USA
[2]Department of Electrical Engineering, University of Babylon, Babylon, Iraq
[†]These authors contributed equally to this paper.
*Corresponding authors. E-mail: wenli@egr.msu.edu, ldong@egr.msu.edu

ers. However, the requirement of acid treatments makes this method incompatible with microelectronics manufacturing. Very recently, the atomic layer etching of graphene was also reported by oxidization of carbon sp^2 bonds to sp^3 bonds with oxygen radicals and the consequent bombardment with argon atoms [22]. Although this technique allowed for a single sheet of graphene to be removed, a large number of defects were introduced to the graphene due to the combination of radical oxidation and argon atom bombarding.

In this study, we developed a simpler and less invasive method for engineering the number of graphene layers using pure oxygen plasma etching. By carefully tuning the variables of the oxygen plasma etching (e.g. power, oxygen flow rate, operating pressure and process duration), we were able to achieve single sheet etching (SSE) of graphene thin films, which removed one single graphene sheet at a time, with both the oxygen reactive ion etching and oxygen plasma etching. Because plasma strength at the ground electrode is lower than that at the powered electrode, the SSE by oxygen plasma can potentially introduce a relatively smaller number of defects to graphene. As a technical demonstration, monolayer graphene has been produced from bilayer graphene by the SSE method. It should be noted that defect formation by oxygen plasma is inevitable even with indirectly coupled gentle oxygen plasma [23], which can significantly affect graphene properties, such as electrical, optical, and thermopower properties [23-27]. To address this issue, we also demonstrated post-etch annealing treatment that can effectively restore disordered graphene. Our process is completely compatible with microelectronics manufacturing and shows the prospect of being a promising post-synthesis method for engineering the number of graphene layers and producing thin graphene films with both large size and high quality.

Methods

Graphenes were first produced with mechanical exfoliation from highly oriented pyrolytic graphite (HOPG) flakes and then transferred onto a Si substrate with a 300 nm thick SiO_2 layer [28]. Optical microscope and micro-Raman spectrograph (Holo Probe Micro-Raman Spectrograph) were used to locate and identify both monolayer and bilayer graphenes. The micro-Raman spectrograph used in this study has an excitation wavelength of 532 nm, a minimal laser spot size of ~5 μm for a 100× magnification, and a power of 0.53 mW. Prior to oxygen plasma etching, all samples were cleaned with acetone rinse for 5 minutes, followed by thermal cleaning in an argon and hydrogen environment. Acetone is used to remove tape residues and other organic contaminations. No chemical effects on graphene at room temperature have been reported in previous literatures. Following the acetone cleaning, the graphene samples were rinsed with isopropanol alcohol and then DI water to remove the acetone residue. We believe that the chemical effect on graphene doping can be negligible. The heat treatment has been shown to effectively remove unavoidable contaminations (e.g. tape residues, resist residues, and adsorbed water) from the as-produced graphene surfaces [29,30]. In our experiments, the treatment was carried out in Ar/H_2 (3% H_2 in volume percentage) atmosphere, with a continuous

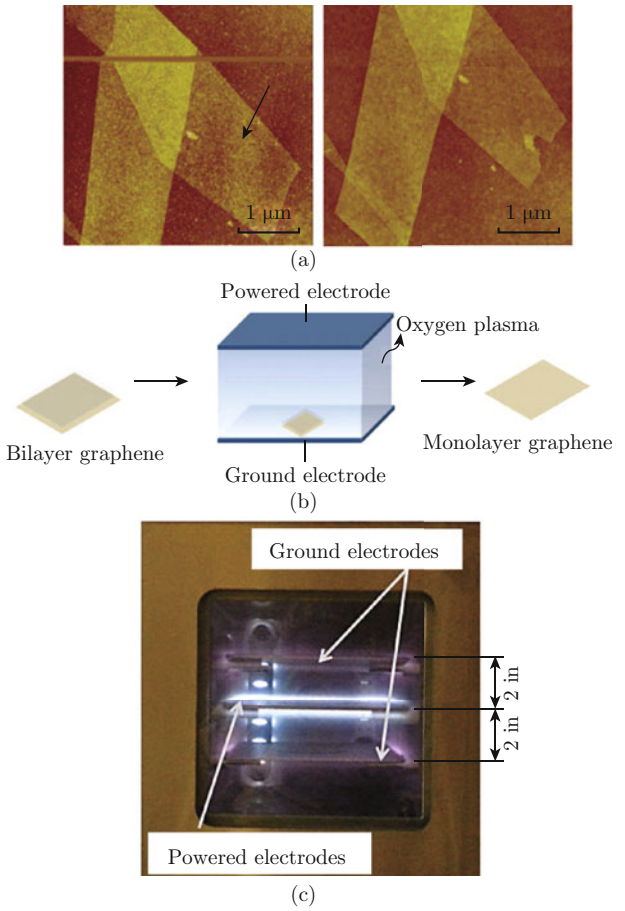

Fig. 1 (a) AFM images of the as-produced monolayer graphene on a SiO_2/Si substrate (left panel), and the corresponding monolayer graphene after the contamination removing thermal treatment, showing the cleaned and smooth graphene surface (right panel). The arrow marks the monolayer graphene region. (b) Schematic cartoon shows the layer engineering process with oxygen plasma. The etching process can be performed with either the oxygen plasma at the ground electrode or the powered electrode. Since the strengths of oxygen plasma at the two electrodes are different, the etching effects on graphene may vary. (c) Experimental setup shows the ground and powered electrodes, which are made of aluminum and have dimensions of 7 in. ×8 in. ×0.093 in. The distance between a ground electrode and the powered one is 2 in. It is clear that the intensity of plasma is higher in the powered electrode than the ground ones based on the brightness.

gas flow of 2000 sccm at 380°C for 40 minutes. As a demonstration of the cleaning efficacy, the left panel in Fig. 1(a) shows the AFM (atomic force microscope, DI 3100) image of the as-produced monolayer graphene that was identified with Raman spectroscopy. Fine granular like particles and contaminations were observed on both the graphene and the SiO_2/Si substrate surfaces. These particles can be effectively removed by heating the as-produced sample in Ar/H_2 atmosphere, as indicated in the right panel of Fig. 1(a).

The SSE of graphene with oxygen plasma was conducted in a plasma etching system (March, PX-250) under the following conditions: RF (radio frequency) of 13.56 MHz, RF power of 70 W, oxygen flow rate of 10 sccm (standard cubic centimeter per minute), base pressure of 70 mTorr, and processing pressure of 313-326 mTorr. These parameters were specifically chosen in order to ignite stable oxygen plasma while reducing plasma strength to minimize plasma induced structural damages and disorders of graphene. During the experiments, the graphene samples were placed on the ground electrode for etching, as schematically displayed in Fig. 1(b). Specifically, the powered electrode refers to the electrode plate that is connected to an RF bias, while the ground electrode plate is connected to the inner wall of the vacuum chamber and also the ground of the etching system. Figure 1(c) shows the experimental setup. The ground and powered electrodes are made of aluminum and have dimensions of 7 in. ×8 in. ×0.093 in. The distance between a ground electrode and the powered one is 2 in. It is clear that the intensity of plasma is higher in the powered electrode than the ground ones based on the brightness. The gentle plasma generated on the ground electrode explains why it required longer time to etch a single layer and generated fewer defects as confirmed later.

The process durations for single sheet removal of graphene were carefully tuned after a large number of experiments and varied according to the location of graphene samples (at powered electrode or ground electrode). AFM and SEM (scanning electron microscopy, Hitachi-4700) were used to inspect the surface topologies of graphene samples before and after being treated with oxygen plasma. Micro-Raman spectroscopy was used to identify the number of graphene layers as well as to study quantitatively the defects of the plasma treated graphene samples.

Results and discussion

SSE of graphene with ground electrode oxygen plasma

In order to characterize the process parameters for SSE of graphene, both monolayer and bilayer graphene films were subjected to oxygen plasma etching for different etching durations. The etching time was increased by a step of 2 seconds. AFM, SEM and Raman spectroscopy were used to investigate graphene topologies after each treatment. Figure 2 shows the evolution of a graphene sample treated by the SSE process with ground oxygen plasma for an optimum process duration of 38 seconds. In this case, the graphene sample hada step with a monolayer region and a bilayer region, which were identified with micro-Raman spectroscopy (Fig. 2(a)). After one SSE step, the monolayer region was completely removed, while the bilayer region was thinned down to a monolayer graphene, as shown in Fig. 2(b). By carefully comparing Figs. 2(a) and 2(b), it can be seen that the border (the upper edge) of the bilayer region did not change obviously, which implies that the edges are not a preferred direction during the etching process. After the second etching, the bilayer region was completely etched away (Fig. 2(c)), leaving the SiO_2/Si substrate. All SEM images were taken at the same location of the sample after each oxygen plasma treatment. Graphene residues were found at the boundary between the monolayer and bilayer regions. This was mainly caused by graphene fragments and folded graphene edges, resulting in thicker graphene areas (> 2 layers).

To further demonstrate the repeatability and controllability of the SSE method with the ground electrode plasma, we applied the optimum recipe to multiple bilayer graphene samples and successfully obtained monolayer graphene films from the bilayer ones, verified by

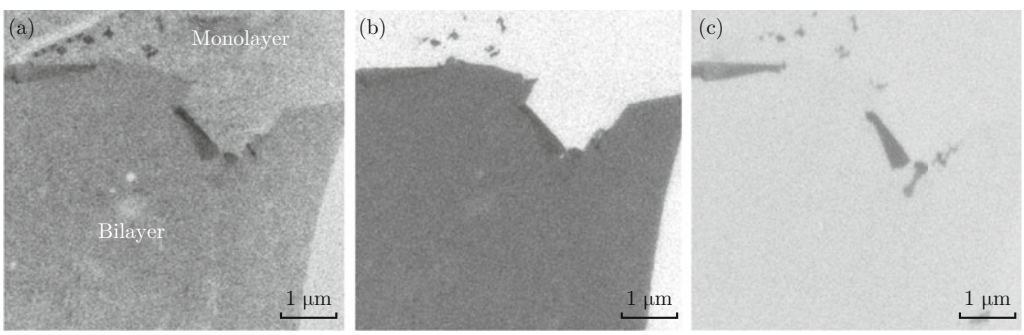

Fig. 2 SEM images show the evolution of a graphene sample after each SSE process with ground electrode oxygen plasma: (a) As-produced; (b) After the first SSE process; (c) After the second SSE process.

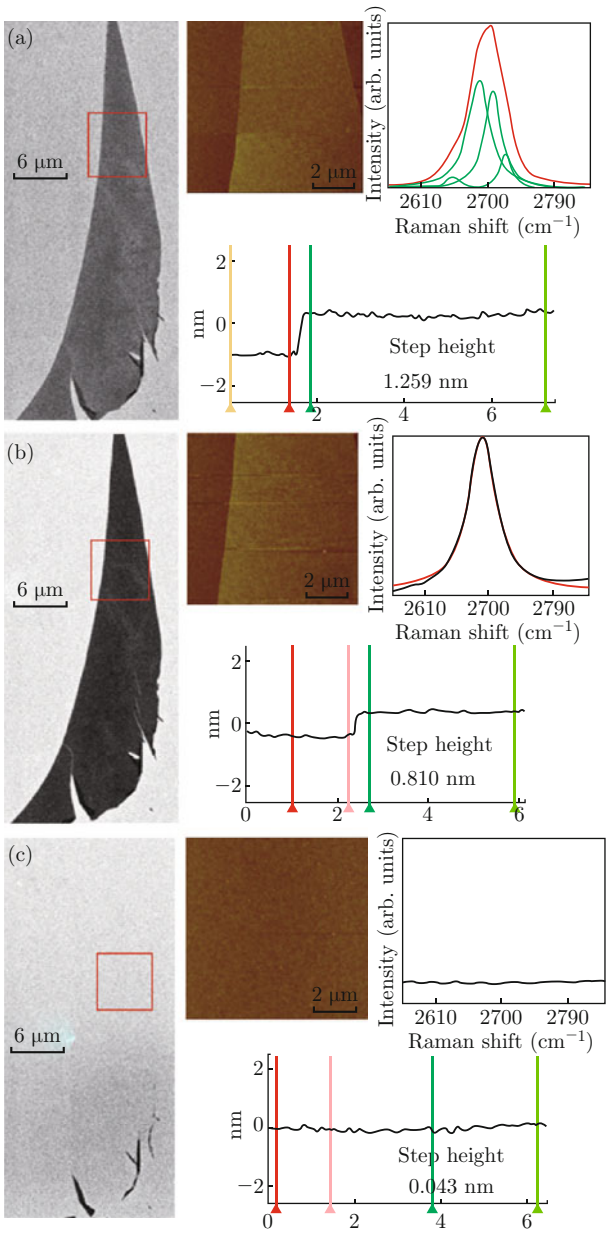

Fig. 3 Demonstration of producing a monolayer graphene from a bilayer graphene with the oxygen plasma etching. Illustrations (a), (b), and (c) show the SEM image, the AFM image (upper left panel), the 2D band of its Raman spectrum (upper right panel) and its height profile from the AFM image (bottom panel) before being etched with oxygen plasma (a), after the first (b) and the second (c) SSE treatments, respectively. Specific regions from which the AFM images and Raman spectra were taken are highlighted by the red squares.

AFM and Raman spectroscopy. Figure 3 shows the evolution of a representative bilayer sample when being subjected to the SSE process. After the first etching (Fig. 3(b)), while the SEM and AFM images had no distinguishable difference between the untreated graphene and the treated one, their Raman spectra and AFM profiles clearly showed the changes resulting from plasma etching. Particularly, the thickness of the bilayer graphene decreased from ~1.259 nm to ~0.810 nm, resulting an apparent difference of 0.449 nm. Graphene thickness measurement using an AFM is typically not atomically precise due to sample contamination and/or an unclean or worn AFM cantilever. The step size 0.449 nm is slightly larger than 0.335 nm (one layer) but obviously much smaller than 0.670 nm (two layers), indicating one atomic carbon layer was removed. The 2D band of its Raman spectrum comprised only one Lorenzian peak, which is another indicator of a monolayer graphene [31,32]. After the second treatment (Fig. 3(c)), the SEM and AFM images taken from the same regions indicate that the bilayer graphene was completely removed with only folded thicker portions of the graphene left on the substrate. This was further confirmed with the Raman spectrum taken from the same location, which contained no specific peak of graphene.

Etching mechanism of oxygen plasma

We have demonstrated that the SSE of graphene can be realized with the oxygen plasma, but it still remains unclear how the oxygen plasma interacts with graphenes. An answer to that question is essential for further understanding the effects of oxygen plasmaon the remaining graphene sheets after the etching process. Two possible etching mechanisms include isotropic etching and anisotropic etching. If the single sheet removal of graphenes by oxygen plasma is isotropic, the etching rate should be uniform everywhere on a graphene sheet regardless of graphene defects and edges. Initiatively, when a single atomic layer is removed from the top, a single or a couple of chains of atoms at the edge will be removed. This is because removing an atom from the top will need sufficient energy to break three bonds, while at the edges, only one or two bonds need to be broken due to the existence of dangling bonds. That means the etching cannot be an isotropic process. For graphene sheets, there are two possible preferred directions for anisotropic etching: vertical (top surface) and horizontal (edges). Experimentally, it is possible to detect a removed single layer using Raman or optical microscopy, but the loss of a couple of chains of atoms at the edge is beyond the resolution of these instruments. Consequently, the sizes of the graphene sheet and the defective regions will not change during the etching in the case of anisotropically vertical etching, but will be projected to the bottom graphene sheet after the etching process, as illustrated in Fig. 4(a). While in the anisotropically horizontal etching mode, the etching rates at the graphene edges and defective regions are anticipated to be higher than that at other intact regions since the edges/defects of graphene tend to react faster with chemicals (e.g.

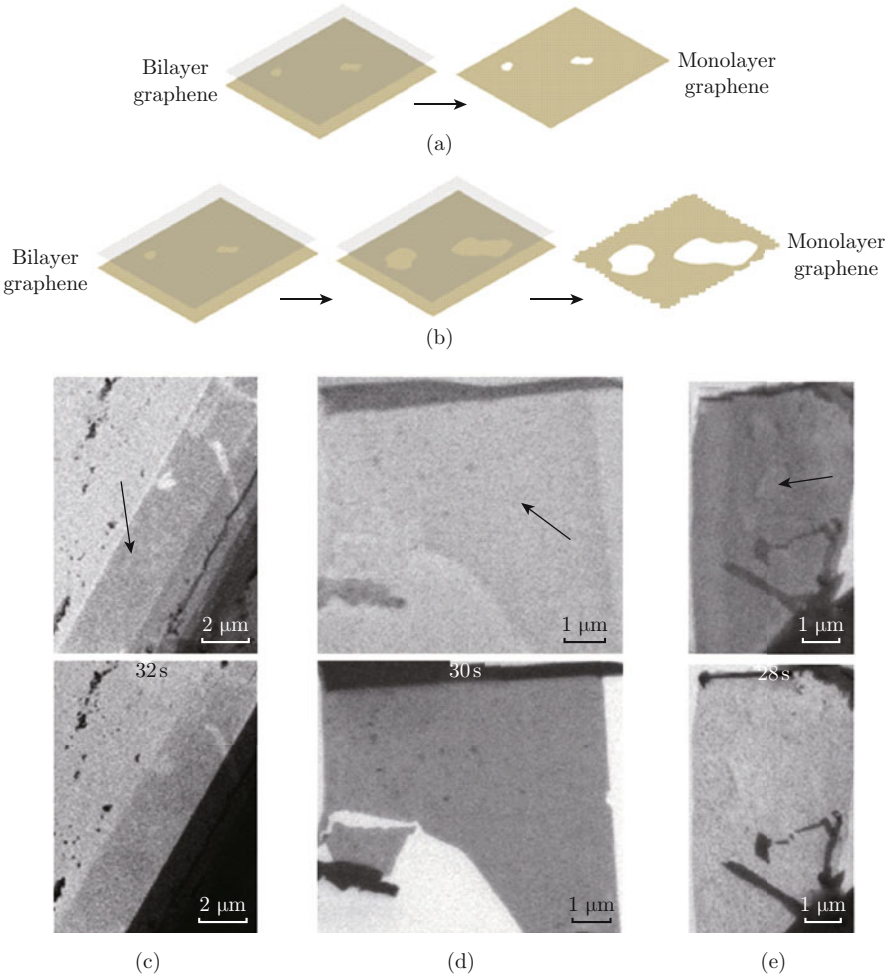

Fig. 4 Schematic cartoons show two possible etching mechanisms of ground electrode oxygen plasma: (a) Anisotropic vertical etching; (b) Anisotropical horizontal etching. In the anisotropic vertical etching mode, the defect patterns on the top graphene sheet will be copied to the bottom graphene sheet with similar sizes. However, in the anisotropical horizontal etching mode, the defect patterns will expand during etching and be copied to the bottom graphene sheet in an obviously. (c)-(e) SEM images of monolayer graphene samples before and after being subjected to oxygen plasma etching for 32 s, 30 s and 28 s, respectively. The monolayer regions of the graphene samples were marked with arrows. In each sub-figure, the top and bottom SEM images show the graphene sample before and after being etched with the corresponding process duration, respectively.

oxygen plasma) than pristine graphene [33]. As schematically displayed in Fig. 4(b), the defective regions of the top graphene sheet will expand, resulting in larger defective areas on the bottom sheet after the etching process. Additionally, the size of the graphene sheet will shrink due to the anisotropic etching of oxygen plasma.

Experiments were conducted in order to investigate which one of these two possible mechanisms will better explain the single sheet removal of graphene. In this study, the etching rate of graphene was relatively fast and the time interval was too short, making it difficult to control the etching time accurately on the same graphene sheet. Therefore, different monolayer graphene samples were etched for various plasma durations and inspected with SEM to evaluate the time evolution of oxygen plasma etching. Etching conditions, such as RF power, oxygen flow rate and working pressure, except the process duration, were kept the same for each sample. Figures 4(c)-(e) show the SEM images of three monolayer graphene samples before and after being etched by the oxygen plasma at the ground electrode with the plasma durations ranging from 28 to 32 seconds. It can be seen that, first, no noticeable area expansions of defective regions in the monolayer samples were observed during the etching. Second, no remarkable shrinkage of the monolayer graphene dimensions due to the possible faster etching rates at the graphene edges was observed during the etching processes. These results suggest that the single sheet removal of graphenes by oxygen plasma is most likely anisotropically vertical etching.

Comparison of the oxygen plasma etching and the oxygen reactive ion etching

With a similar means of investigation, singular layer etching of graphene can also be achieved with oxygen reactive ion etching at the powered electrode for a shorter etching duration of 17 seconds. Figure 5 provides the demonstration of a monolayer graphene produced from a bilayer graphene using the oxygen reactive ion etching. A ~0.4 nm thickness decrease of the graphene was observed after one SSE plasma treatment. The evolution of its Raman 2D band also demonstrated that a monolayer graphene was produced from the bilayer graphene.

It is known that the strength of oxygen plasma varies at the powered electrode and the ground electrode (as shown in Fig. 1(c)), which is anticipated to result in different levels of physical damage and defects on the post-etch graphene sheets. Therefore, we investigated the plasma induced defects on a variety of plasma-treated graphene samples by measuring the intensity ratios of the D band and G band (I_D/I_G) in their Raman spectra. A higher I_D/I_G ratio indicates a larger number of defects. Figure 6(a) and 6(b) show the Raman spectra taken from two bilayer graphene samples before and after SSE by the oxygen reactive ion etching and the oxygen plasma etching, respectively. The Raman spectra show that the sample etched with the oxygen reactive ion etching at the powered electrode had an I_D/I_G ratio of ~1.18 (the bottom panel of Fig. 6(a)), while the I_D/I_G ratio of the graphene etched with the oxygen plasma at the ground electrode was ~0.94 (the bottom panel of Fig. 6(b)). The statistical analysis of the Raman I_D/I_G ratios of multiple plasma treated samples was summarized in Fig. 6(c). The average I_D/I_G ratio of graphene samples after etching with the powered electrode oxygen plasma was ~1.05, while the average I_D/I_G ratio after etching with the oxygen plasma was ~0.86. These results indicate that the oxygen plasma introduced fewer defects compared to the powered electrode oxygen plasma, which is mainly due to the relatively low strength of oxygen plasma at the ground electrode.

Furthermore, it is found that the amount of defects can be reduced significantly with a post-etch annealing treatment. The annealing process was carried out in an Ar environment at 900-1000°C for 1 h. Figure 6(d) shows the Raman spectrum of a monolayer graphene, which was produced with the SSE method, after the annealing process. Compared with its Raman spectrum before the annealing process, which was shown in the bottom panel of Fig. 6(a), it can be seen that the intensity of the D band peak has been greatly suppressed by the annealing process. The recovery of disordered graphene by high temperature Ar annealing may be

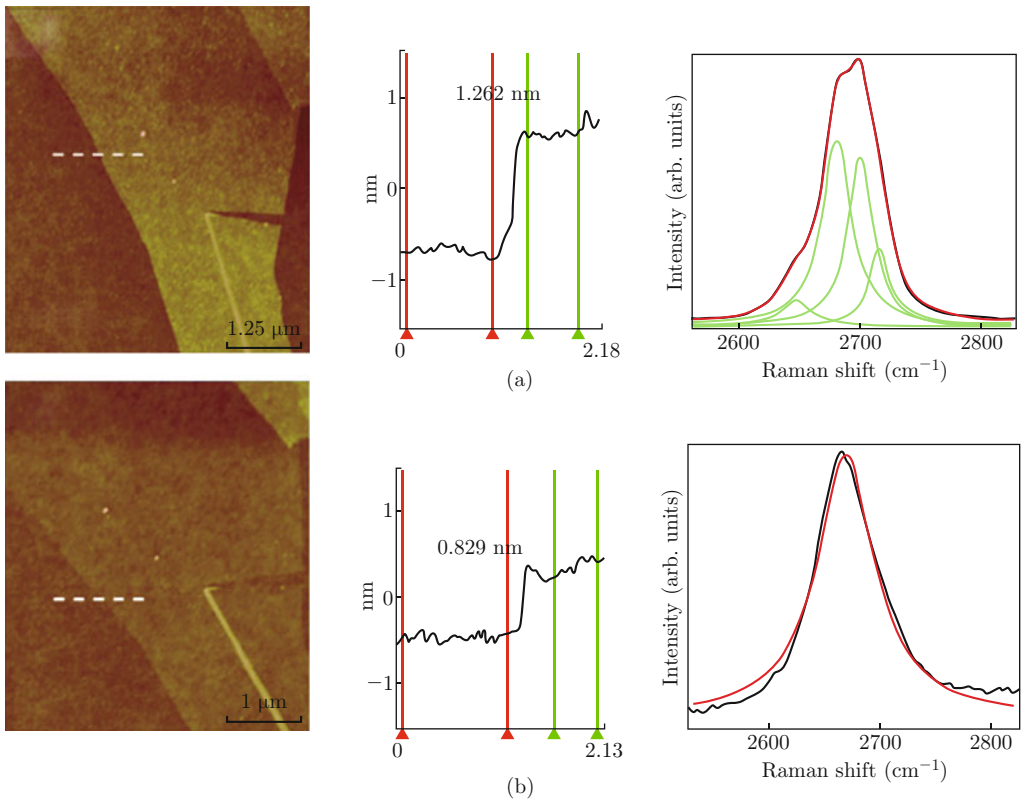

Fig. 5 AFM images, height profiles and the 2D bands of its Raman spectrum of a bilayer graphene (a) Before and (b) After the SSE with powered electrode oxygen plasma, demonstrating the production of a monolayer graphene from a bilayer graphene.

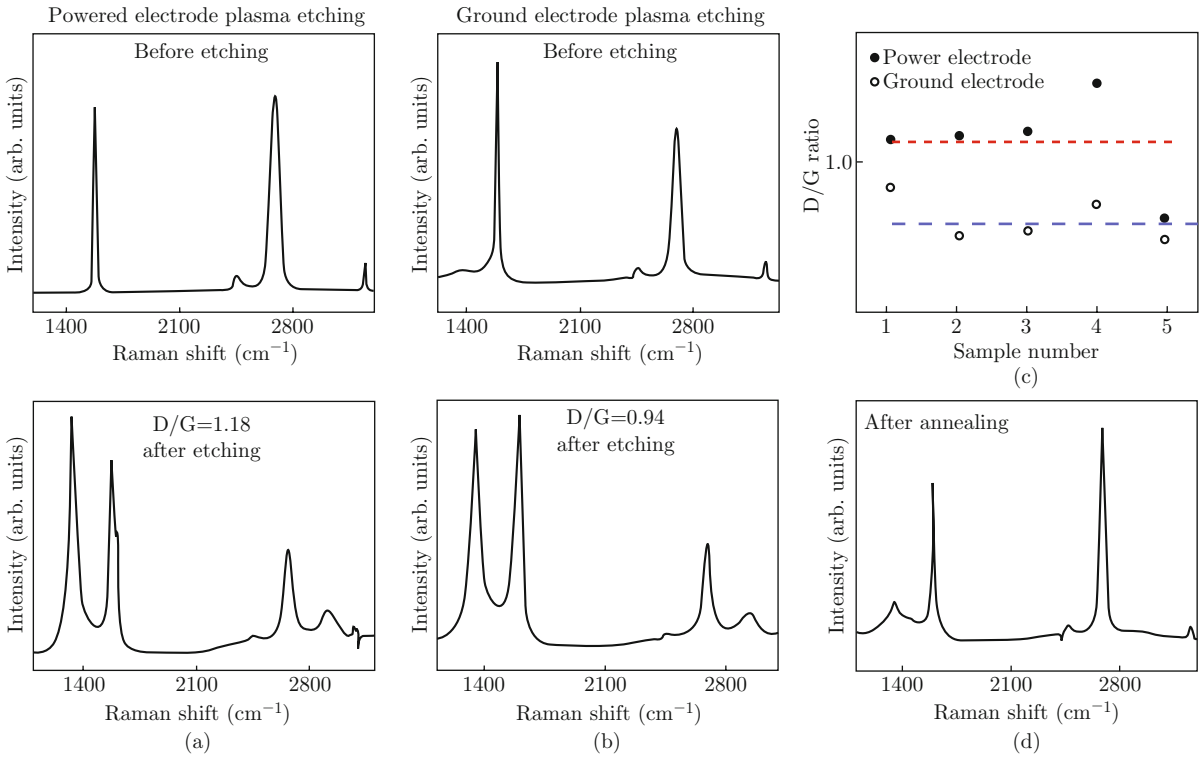

Fig. 6 Raman spectra of bilayer graphene samples before and after the SSE process with (a) the powered electrode oxygen plasma and (b) the ground electrode oxygen plasma. (c) Statistic analysis of Raman I_D/I_G ratios of graphene samples after being etched with the powered electrode (solid circles) and the oxygen plasma (open circles). The red and blue dotted lines show the average values of data from solid and open circles, respectively. (d) Raman spectrum of the monolayer graphene produced from a bilayer graphene after the annealing treatment. Its Raman spectrum before annealing is shown in the bottom panel of (a).

related to the thermally induced reconstruction of graphene lattice and dangling bonds [34] as well as graphene dehydrogenation [35]. It should be mentioned that electron beam irradiation during the SEM step is known to have effects on the transformation of the crystalline order and electronic properties of mono/bilayer graphene films [36]. During our quantitative studies of defects, the as-etched graphene samples were examined only by the micro-Raman spectroscopy in order to eliminate additional defect formation due to the electron beam irradiation. Therefore, the formation and partial recovery of defects on our graphene substrates are mainly attributed to the oxygen plasma etching and their successive annealing treatment.

Fabrication of suspended graphene

Our method can also be applied in controlling the number of layers in the case of suspended graphene. In this approach, tranches were made on the SiO_2 (300 nm)/Si substrates through photolithography and induced coupled plasma reactive ion etching (ICP-RIE), respectively. First, SiO_2 was completely removed and Si substrate was etched down by around 10 μm. Next, graphene layer was prepared using micro mechanical exfoliation and then deposited over the tranches and the holes. After that, graphenes were located by optical microscope and Raman spectroscope. Then graphene layer was etched layer-by-layer using oxygen plasma, showing that the SSE method provides a possible way to produce graphenes directly from graphite flakes. Figure 7 shows a suspended graphene sheet with a thickness of ∼2 nm produced through layer by layer etching of a graphite flake of an original thickness of ∼15 nm.

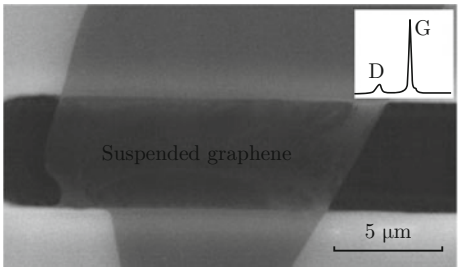

Fig. 7 SEM image of a suspended graphene sample of 2 nm thickness produced from graphite flake of ∼ 15 nm using layer by layer oxygen plasma etching. Inset is the Raman spectra.

Conclusions

In this paper, we developed a method for engineering

the number of graphene layers with oxygen plasma that is simple and compatible with microelectronics manufacturing. SSE processes, which remove only one single graphene sheet at a time, were achieved with both the powered electrode oxygen plasma and the ground electrode oxygen plasma. Production of monolayer graphene films from bilayer graphene samples was demonstrated with our SSE processes. The results show that the oxygen plasma etching of graphene was an anisotropically vertical etching process. It was also found that etching with the oxygen plasma etching introduced fewer defects onto the bottom graphene layer compared with oxygen reactive ion etching. That is because the oxygen plasma strength was lower at the ground electrode than at the powered electrode. The plasma induced defects can be obviously suppressed by an annealing process after oxygen plasma etching. Our results provide a post-synthesis approach to the single sheet precision subtraction of graphene layers and the possibility of producing large size graphene thin films directly from multilayer graphene or even graphite flakes. These films can be used for constructing novel graphene based devices by selectively etching the graphene at specific regions.

References

[1] A. K. Geim, "Graphene: Status and prospects", Science 324(5934), 1530-1534 (2009). http://dx.doi.org/10.1126/science.1158877

[2] X. Du, I. Skachko, A. Barker and E. Y. Andrei, "Approaching ballistic transport in suspended graphene", Nature Nanotech. 3(8), 491-495 (2008). http://dx.doi.org/10.1038/nnano.2008.199

[3] K. S. Novoselov, Z. Jiang, Y. Zhang, S. V. Morozov, H. L. Stormer, U. Zeitler, J. C. Maan, G. S. Boebinger, P. Kim and A. K. Geim, "Room-temperature quantum hall effect in graphene", Science 315(5817), 1379-1379 (2007). http://dx.doi.org/10.1126/science.1137201

[4] A. K. Geim and K. S. Novoselov, "The rise of graphene", Nat. Mater. 6(3), 183-191 (2007). http://dx.doi.org/10.1038/nmat1849

[5] C. N. R. Rao, A. K. Sood, K. S. Subrahmanyam and A. Govindaraj, "Graphene: The new two-dimensional nanomaterial", Angew. Chem. Int. Edit.48 (42), 7752-7777 (2009). http://dx.doi.org/10.1002/anie.200901678

[6] F. Schwierz, "Graphene transistors", Nature Nanotech. 5(7), 487-496 (2010). http://dx.doi.org/10.1038/nnano.2010.89

[7] M. Wanunu, T. Dadosh, V. Ray, J. M. Jin, L. McReynolds and M. Drndic, "Rapid electronic detection of probe-specific microRNAs using thin nanopore sensors", Nature Nanotech. 5(11), 807-814 (2010). http://dx.doi.org/10.1038/nnano.2010.202

[8] F. Schedin, A. K. Geim, S. V. Morozov, E. W. Hill, P. Blake, M. I. Katsnelson and K. S. Novoselov, "Detection of individual gas molecules adsorbed on graphene", Nat. Mater. 6(9), 652-655 (2007). http://dx.doi.org/10.1038/nmat1967

[9] Y. W. Zhu, S. Murali, M. D. Stoller, K. J. Ganesh, W. W. Cai, P. J. Ferreira, A. Pirkle, R. M. Wallace, K. A. Cychosz, M. Thommes, D. Su, E. A. Stach and R. S. Ruoff, "Carbon-based supercapacitors produced by activation of graphene", Science 332(6037), 1537-1541 (2011). http://dx.doi.org/10.1126/science.1200770

[10] S. Stankovich, D. A. Dikin, G. H. B. Dommett, K. M. Kohlhaas, E. J. Zimney, E. A. Stach, R. D. Piner, S. T. Nguyen and R. S. Ruoff, "Graphene-based composite materials", Nature 442(7100), 282-286 (2006). http://dx.doi.org/10.1038/nature04969

[11] K. V. Emtsev, A. Bostwick, K. Horn, J. Jobst, G. L. Kellogg, L. Ley, J. L. McChesney, T. Ohta, S. A. Reshanov, J. Rohrl, E. Rotenberg, A. K. Schmid, D. Waldmann, H. B. Weber and T. Seyller, "Towards wafer-size graphene layers by atmospheric pressure graphitization of silicon carbide", Nat. Mater. 8(3), 203-207 (2009). http://dx.doi.org/10.1038/nmat2382

[12] X. S. Li, W. W. Cai, J. H. An, S. Kim, J. Nah, D. X. Yang, R. Piner, A. Velamakanni, I. Jung, E. Tutuc, S. K. Banerjee, L. Colombo and R. S. Ruoff, "Large-area synthesis of high-quality and uniform graphene films on copper foils", Science 324(5932), 1312-1314 (2009). http://dx.doi.org/10.1126/science.1171245

[13] S. Bae, H. Kim, Y. Lee, X. F. Xu, J. S. Park, Y. Zheng, J. Balakrishnan, T. Lei, H. R. Kim, Y. I. Song, Y. J. Kim, K. S. Kim, B. Ozyilmaz, J. H. Ahn, B. H. Hong and S. Iijima, "Roll-to-roll production of 30-inch graphene films for transparent electrodes", Nature Nanotech. 5(8), 574-578 (2010). http://dx.doi.org/10.1038/nnano.2010.132

[14] X. L. Li, H. L. Wang, J. T. Robinson, H. Sanchez, G. Diankov and H. J. Dai, "Simultaneous nitrogen doping and reduction of graphene oxide", J. Am. Chem. Soc. 131(43), 15939-15944 (2009). http://dx.doi.org/10.1021/ja907098f

[15] F. B. Rao, H. Almumen, Z. Fan, W. Li and L. X. Dong, "Inter-sheet-effect-inspired graphene sensors: design, fabrication and characterization", Nature Nanotech. 23(10), 105501 (2012). doi:10.1088/0957-4484/23/10/105501

[16] Y. B. Zhang, T. T. Tang, C. Girit, Z. Hao, M. C. Martin, A. Zettl, M. F. Crommie, Y. R. Shen and F. Wang, "Direct observation of a widely tunable bandgap in bilayer graphene", Nature 459(7248), 820-823 (2009). http://dx.doi.org/10.1038/nature08105

[17] G. X. Zhao, D. D. Shao, C. L. Chen and X. K. Wang, "Synthesis of few-layered graphene by H_2O_2 plasma etching of graphite", Appl. Phys. Lett. 98(18), 183114 (2011). http://dx.doi.org/10.1063/1.3589354

[18] H. M. Wang, Y. H. Wu, Z. H. Ni and Z. X. Shen, "Electronic transport and layer engineering in multilayer

graphene structures", Appl. Phys. Lett. 92(5), 053504 (2008). http://dx.doi.org/10.1063/1.2840713

[19] C. X. Cong, T. Yu, H. M. Wang, K. H. Zheng, P. Q. Gao, X. D. Chen and Q. Zhang, "Self-limited oxidation: A route to form graphene layers from graphite by one-step heating", Small 6(24), 2837-2841 (2010). http://dx.doi.org/10.1002/smll.201001184

[20] K. S. Hazra, J. Rafiee, M. A. Rafiee, A. Mathur, S. S. Roy, J. McLauhglin, N. Koratkar and D. S. Misra, "Thinning of multilayer graphene to monolayer graphene in a plasma environment", Nature Nanotech. 22(2), 025704 (2011). http://dx.doi.org/10.1088/0957-4484/22/2/025704

[21] A. Dimiev, D. V. Kosynkin, A. Sinitskii, A. Slesarev, Z. Z. Sun and J. M. Tour, "Layer-by-layer removal of graphene for device patterning", Science 331(6021), 1168-1172 (2011). http://dx.doi.org/10.1126/science.1199183

[22] W. S. Lim, Y. Y. Kim, H. Kim, S. Jang, N. Kwon, B. J. Park, J. H. Ahn, I. Chung, B. H. Hong and G. Y. Yeom, "Atomic layer etching of graphene for full graphene device fabrication", Carbon 50(2), 429-435 (2012). http://dx.doi.org/10.1016/j.carbon.2011.08.058

[23] D. C. Kim, D. Y. Jeon, H. J. Chung, Y. Woo, J. K. Shin and S. Seo, "The structural and electrical evolution of graphene by oxygen plasma-induced disorder", Nature Nanotech. 20(37), 375703 (2009). http://dx.doi.org/10.1088/0957-4484/20/37/375703

[24] A. Nourbakhsh, M. Cantoro, T. Vosch, G. Pourtois, F. Clemente, M. H. van der Veen, J. Hofkens, M. M. Heyns, S. De Gendt and B. F. Sels, "Bandgap opening in oxygen plasma-treated graphene", Nature Nanotech. 21(43), 435203 (2010). doi:10.1088/0957-4484/21/43/435203

[25] A. Nourbakhsh, M. Cantoro, A. V. Klekachev, G. Pourtois, T. Vosch, J. Hofkens, M. H. van der Veen, M. M. Heyns, S. De Gendt and B. F. Sels, "Single layer vs bilayer graphene: a comparative study of the effects of oxygen plasma treatment on their electronic and optical properties", J. Phys. Chem. C. 115(33), 16619-16624 (2011). http://dx.doi.org/10.1021/jp203010z

[26] T. Gokus, R. R. Nair, A. Bonetti, M. Bohmler, A. Lombardo, K. S. Novoselov, A. K. Geim, A. C. Ferrari and A. Hartschuh, "Making graphene luminescent by oxygen plasma treatment", ACS Nano 3(12), 3963-3968 (2009). http://dx.doi.org/10.1021/nn9012753

[27] N. Xiao, X. C. Dong, L. Song, D. Y. Liu, Y. Tay, S. X. Wu, L. J. Li, Y. Zhao, T. Yu, H. Zhang, W. Huang, H. H. Hng, P. M. Ajayan and Q. Y. Yan, "Enhanced thermopower of graphene films with oxygen plasma treatment", ACS Nano 5(4), 2749-2755 (2011). http://dx.doi.org/10.1021/nn2001849

[28] P. Blake, E. W. Hill, A. H. C. Neto, K. S. Novoselov, D. Jiang, R. Yang, T. J. Booth and A. K. Geim, "Making graphene visible", Appl. Phys. Lett. 91(6), 063124 (2007). http://dx.doi.org/10.1063/1.2768624

[29] M. Ishigami, J. H. Chen, W. G. Cullen, M. S. Fuhrer and E. D. Williams, "Atomic structure of graphene on SiO_2", Nano Lett. 7(6), 1643-1648 (2007). http://dx.doi.org/10.1021/nl070613a

[30] L. C. Campos, V. R. Manfrinato, J. D. Sanchez-Yamagishi, J. Kong and P. Jarillo-Herrero, "Anisotropic etching and nanoribbon formation in single-layer graphene", Nano Lett. 9(7), 2600-2604 (2009). http://dx.doi.org/10.1021/nl900811r

[31] A. C. Ferrari, J. C. Meyer, V. Scardaci, C. Casiraghi, M. Lazzeri, F. Mauri, S. Piscanec, D. Jiang, K. S. Novoselov, S. Roth and A. K. Geim, "Raman spectrum of graphene and graphene layers", Phys. Rev. Lett. 97(18), 187401 (2006). http://dx.doi.org/10.1103/PhysRevLett.97.187401

[32] D. Graf, F. Molitor, K. Ensslin, C. Stampfer, A. Jungen, C. Hierold and L. Wirtz, "Spatially resolved raman spectroscopy of single- and few-layer graphene", Nano Lett. 7(2), 238-242 (2007). http://dx.doi.org/10.1021/nl061702a

[33] M. Batzill, "The surface science of graphene: Metal interfaces, CVD synthesis, nanoribbons, chemical modifications, and defects", Surf. Sci. Rep. 67(3-4), 83-115 (2012). http://dx.doi.org/10.1016/j.surfrep.2011.12.001

[34] J. Campos-Delgado, Y. A. Kim, T. Hayashi, A. Morelos-Gomez, M. Hofmann, H. Muramatsu, M. Endo, H. Terrones, R. D. Shull, M. S. Dresselhaus and M. Terrones, "Thermal stability studies of CVD-grown graphene nanoribbons: Defect annealing and loop formation", Chem. Phys. Lett. 469(1-3), 177-182 (2009). http://dx.doi.org/10.1016/j.cplett.2008.12.082

[35] D. C. Elias, R. R. Nair, T. M. G. Mohiuddin, S. V. Morozov, P. Blake, M. P. Halsall, A. C. Ferrari, D. W. Boukhvalov, M. I. Katsnelson, A. K. Geim and K. S. Novoselov, "Control of graphene's properties by reversible hydrogenation: evidence for graphane", Science 323(5914), 610-613 (2009). http://dx.doi.org/10.1126/science.1167130

[36] D. Teweldebrhan and A. A. Balandin, "Modification of graphene properties due to electron-beam irradiation", Appl. Phys. Lett. 94(1), 013101 (2009). http://dx.doi.org/10.1063/1.3062851